Materials Letters 166 (2016) 113–115

Contents lists available at ScienceDirect

Materials Letters

journal homepage: www.elsevier.com/locate/matlet

Preparation of spherical and dendritic CdS@TiO_2 hollow double-shelled nanoparticles for photocatalysis

Guanhua Sun [a,b], Chaosheng Zhu [a], Jingtang Zheng [a,*], Bo Jiang [a], Huacheng Yin [a], Han Wang [a], Shi Qiu [a], Jianjun Yuan [a,b], Mingbo Wu [a], Wenting Wu [a], Qingzhong Xue [a]

[a] State Key Laboratory of Heavy Oil Processing, China University of Petroleum, Qingdao 266555, PR China
[b] Lanzhou Branch of Changzheng Engineering Company Limited 730010, PR China

ARTICLE INFO

Article history:
Received 12 August 2015
Received in revised form
12 November 2015
Accepted 28 November 2015
Available online 2 December 2015

Keywords:
Crystal growth
Nanoparticles
Core–shell
Photocatalysis

ABSTRACT

Spherical and dendritic CdS@TiO_2 hollow double-shelled nanoparticles (HDNPs) with visible light photocatalytic activity were synthesized via sol–gel and wet-chemical approach respectively. The morphology, composition, size of the nanoparticles and crystal structure of the synthesized CdS@TiO_2 HDNPs were characterized by XRD, TEM, and SAED. The results showed that morphologies and crystalline phases of as-prepared CdS@TiO_2 HDNPs mainly depended on the synthesis conditions such as temperature and pressure. Compared with the typical core–shell of PS@TiO_2 and PS@CdS, CdS@TiO_2 HDNPs, their photocatalytic activity was obviously enhanced with maximum degradation efficiency of RhB as high as 99.9%.

1. Introduction

In recent years, the core–shell nanoparticles have aroused great interest due to the tremendous demands of modern technology for more advanced materials, particularly in the photocatalysis field [1,2]. Previously researchers synthesized CdS@TiO_2 core–shell structure samples exhibited greatly enhanced photocatalytic activity toward the degradation of Rhodamine B (RhB) and 4-chlorophenol aqueous solution under visible light irradiation ($\lambda > 420$ nm) [3]. The enhanced photosensitivity and catalytic properties of the combination of CdS and TiO_2 resulted from reducing electron-hole recombination rate via photoexcited electron transporting from the TiO_2 shell to the CdS core.

However, in the case of the heterogeneous photocatalytic reaction, low surface-to-volume ratio of solid nanoparticle greatly affects its catalytic effect for containment removal [4]. Recently, hollow microspheres nanomaterials have been proved to be a promising structure to make up for the deficiency with high surface area, low density, excellent loading capacity and high light-harvesting efficiency [5,6].

In this paper, we report an ultrasonic-assisted reaction followed by a subsequent sol–gel or wet-chemical method for preparing CdS@TiO_2 HDNPs with spherical and dendritic morphologies and estimate their photocatalytic performance.

2. Experimental details

2.1. Preparation of spherical and dendritic CdS@TiO_2 HDNPs

The hydrolysate of Ti (VI) source as TiO_2 precursor was coated on PS@CdS in in our previous work [7,8]: As-prepared PS@CdS powder of 0.2 g was ultrasonic dispersed in 50 mL of ethanol and then 0.08 mL of tetrabutyl titanate (TBT) was added into the mixture. Subsequently, the de-ionized water dropwised in the solution above, which next heated at 60 °C for 2 h. To obtain the spherical ones, the solution above needed continual heating at 60 °C for 15 h. To obtain the dendritic ones, the mixture was transferred into hydrothermal reactor and heated at 180 °C for 15 h. At last, the CdS@TiO_2 HDNPs were obtained by calcining at 550 °C for 4 h to remove polymer cores and crystallize TiO_2. As a comparison, we also prepared the PS@TiO_2 core–shell by sol–gel process.

2.2. Material characterization

Microstructural characterizations of the core–shell nanoparticles were carried out by transmission electron microscopy (TEM, JEOL: JEM-2100UHR) operated at an accelerating voltage of 200 kV. Phase determination of the core–shell nanoparticles was carried out by an X-ray diffract meter using Ni-filtered Cu K radiation at 40 kV and 40 mA in the 2θ range of 20–80°, with a scan rate of 0.02° per second (wavelength = 1.54056 Å).

* Corresponding author.
E-mail address: jtzheng03@163.com (J. Zheng).

http://dx.doi.org/10.1016/j.matlet.2015.11.127
0167-577X/

3. Results and discussion

3.1. Structural characterization

Fig. 1 shows the XRD patterns of PS@CdS, PS@TiO_2 core–shell and spherical and dendritic CdS@TiO_2 HDNPs samples and examines the crystallographic structure of the as-prepared samples. A comparison of the XRD patterns of PS@TiO_2 and PS@CdS with two kinds of CdS@TiO_2 HDNPs (blue and red) reveals an increase in the intensity of the TiO_2 peak in CdS@TiO_2 HDNPs and peak at 25.3° so then concluding a successful combination of TiO_2 and CdS nanoparticles in spherical and dendritic CdS@TiO_2 HDNPs. In addition, a typical diffraction peak of anatase's TiO_2, located at $2\theta=25.3°$, is observed in dendritic CdS@TiO_2 HDNPs, which is more intense than spherical one due to its higher content of the (101) crystal plane of anatase-phase TiO_2.

Detailed morphological features and crystallinity of the PS@CdS and CdS@TiO_2 HDNPs were investigated using TEM and SAED analyses, as is shown in Fig. 2. Fig. 2a and b show that the CdS-coated shell thickness was approximately 40 nm and the formation of double shell spherical structures with shells of about 90 nm in thickness. Fig. 2c presents that the growing pattern of TiO_2 nanoparticles changed and adendritic morphology can be distinguished with increasing reaction temperature up to 180 °C. Insets in Fig. 2d and e display the high-resolution TEM (HRTEM) and SAED images of spherical and dendritic CdS@TiO_2 HDNPs. The identified lattice spacings of 0.351, 0.458 and 0.356 nm in HRTEM images of insets in Fig. 2d and e correspond to the (101) plane of anatase TiO_2, (001) plane of rutile TiO_2 and (100) plane of hexagonal CdS phase, respectively.

3.2. Growth mechanism

In this work, we described that the preparation of CdS@TiO_2 HDNPs with sol–gel or wet-chemical method after the ultrasound-assisted synthesis of PS@CdS core–shell structure. The formation mechanism of PS@CdS core–shell structure has been clarified in our previous work [7]. In the growth progress of TiO_2 onto CdS layer surface, the temperature is an important factor of controlling the crystal type and microstructural aspect of TiO_2. The previous studies indicated that TiO_2 nanoparticles were prepared by the sol–gel process from a condensed $Ti(OH)_4$ gel preformed by the hydrolysis of a Ti(VI) source. It took about a few hours or more for hydroxide ions to reach the adsorption equilibrium with $Ti(OH)_4$ precipitate at a lower temperature, but it was promoted and greatly accelerated at a higher temperature [9]. It is a slow and less severe process to form TiO_2 particles at the reaction temperature of 60 °C under atmospheric condition which could form a smooth TiO_2 layer. To gain mixed precursor of TiO_2, the solution was placed under this condition for 2 h in the first step. With the increasing of reaction temperature, as one can imagine, the violence of the reaction gets higher step by step. While reaching 180 °C, the growth of TiO_2 is so fast that the newly generated particles seek to expand. In the case of dendritic CdS@TiO_2 HDNPs, the formation of dendritic TiO_2 nanorods probably attributes to the remainder PVP of extending on the CdS surface and PVP plays a role of surfactant to assist TiO_2 nanorods to extend vertically on the CdS surface. Meanwhile, we discovered that the longer of the reaction time in the hydrothermal process was, the longer of TiO_2 nanorods were.

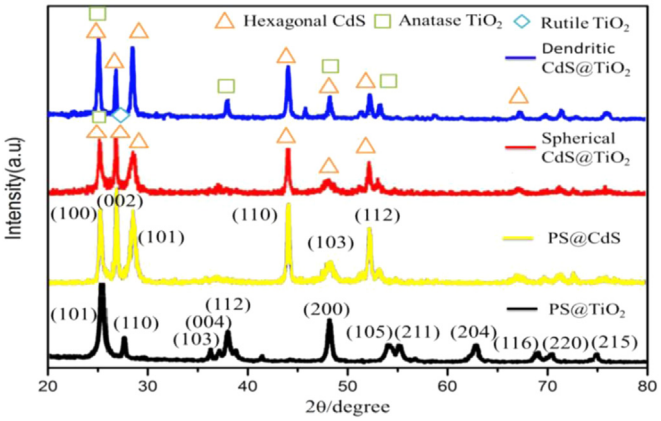

Fig. 1. XRD pattern of PS@TiO_2, PS@CdS core–shell nanoparticles and spherical and dendritic CdS@TiO_2 HDNPs. (For interpretation of the references to color in this figure legend, the reader is referred to the web version of this article.)

3.3. Photocatalysis test

To evaluate the photocatalytic activity of the as-prepared samples, 40 mg of the powder was dispersed in 200 mL deionized water containing 5 mg/L RhB. A 500W Xenon lamp with a cutoff filter ($\lambda > 400$ nm) was used as the visible source. Before each irradiation, the solutions were kept in the dark for 1 h in order to reach the adsorption equilibrium. The photocatalytic performances of the four as-prepared samples have been shown in Fig. 3.

It can be observed obviously that the photocatalytic activity of different catalysts decreased in the following order: dendritic CdS@TiO_2 > PS@CdS > spherical CdS@TiO_2 > PS@TiO_2. The dendritic CdS@TiO_2 HDNPs demonstrated significantly improved photocatalytic performance in comparison with PS@CdS for photocatalytic redox reactions. It was clear that the enhancement of photocatalytic performance of these combined nanoparticles was mainly resulted from the charge transformation at the interfaces between CdS and TiO_2 with matched band structure, which accordingly favored an effective photoexcited electron hole separation in these two layers [10]. The photoinduced electrons on the CdS surface can transfer easily to conduction band (CB) of TiO_2. Likewise, photoinduced holes on the TiO_2 surface will migrate to CdS due to different valence band (VB) edge potentials. However, when the density of the TiO_2 outer shell is reach a high-value, even CdS was entirely covered (spherical CdS@TiO_2), its surface active sites for the holes will be occupied. This moment the surface TiO_2 layer would be excited first by the light and injected electrons into the CB of CdS, causing a suppression of the generation of excitons from CdS, resulting in a lower photocatalytic activity even than pure PS@CdS [11]. For the dendritic CdS@TiO_2 HDNPs, only parts CdS are covered by TiO_2, which exposes more active sites. The dendritic CdS@TiO_2 HDNPs have not only hollow double-shelled structure but also abundant sharp corners and edges and result in higher surface area. By and large, in addition, the anatase of TiO_2 exhibits higher photocatalysis activity than crystal shape of rutile and dendritic samples contain more anatase of TiO_2. The above reasons cooperate to make the dendritic CdS@TiO_2 HDNPs possess the highest photocatalytic effect and superior electrochemical properties compared to other nanoparticles with smooth surfaces.

4. Conclusions

In this work, two novel types of CdS@TiO_2 HDNPs were successfully synthesized based on a strategy of controlling the hydrolysis extent of the precursor of TiO_2 chiefly and tested for their photocatalytic activity. Dendritic CdS@TiO_2 HDNPs exhibited higher photocatalytic activity than PS@CdS core–shell and

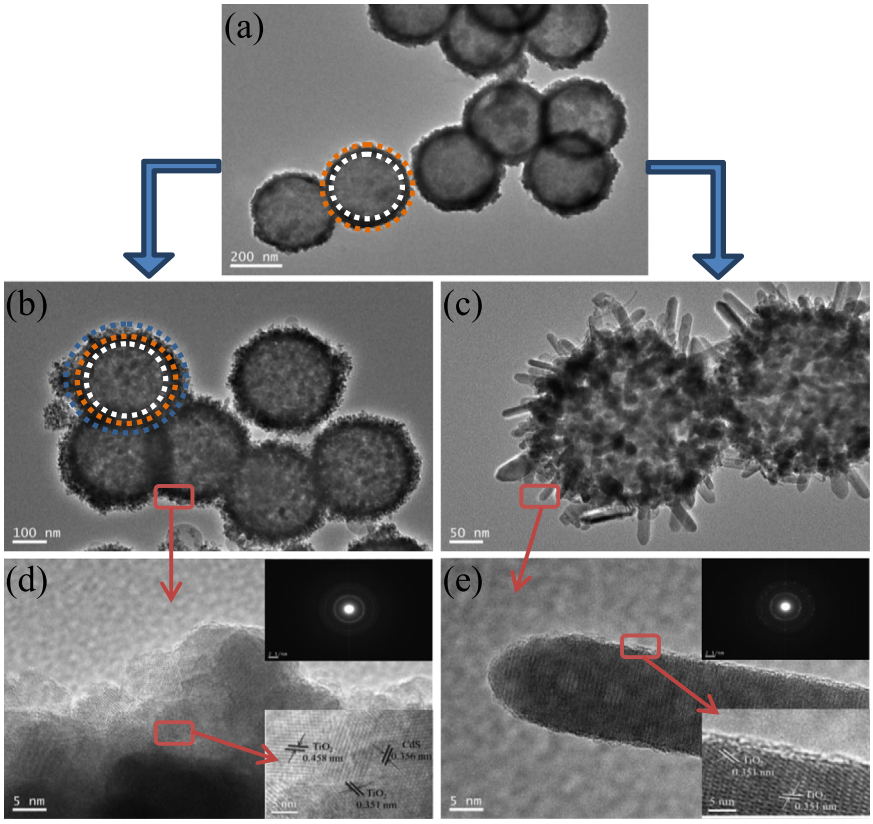

Fig. 2. Typical TEM images of PS@CdS core–shell (a), spherical CdS@TiO_2 HDNPs (b), dendritic CdS@TiO_2 HDNPs (c). High-powered TEM of spherical CdS@TiO_2 HDNPs (d) and dendritic CdS@TiO_2 HDNPs (e).

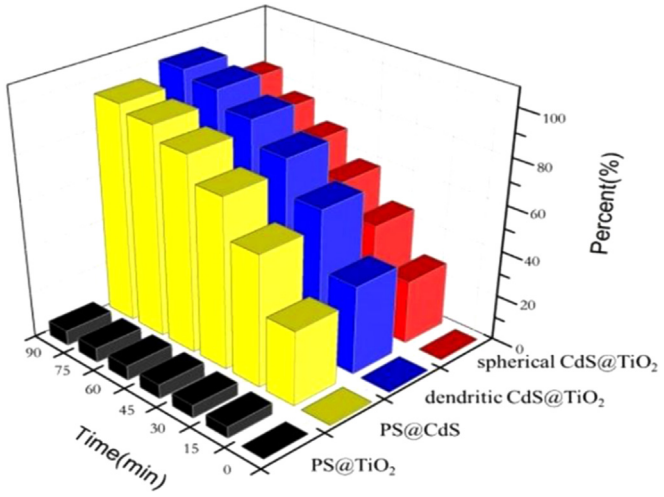

Fig. 3. RhB reduction as a function of illumination time for PS@TiO_2, PS@CdS core–shell nanoparticles and spherical and dendritic CdS@TiO_2 HDNPs.

spherical CdS@TiO_2 HDNPs under visible light. Thus, dendritic CdS@TiO_2 HDNPs are promising materials for application in degradation of dye wastewater. This paper opens up a new way to synthesize CdS@TiO_2 HDNPs and to further improve the photocatalysis performance of CdS@TiO_2-based devices.

Acknowledgments

This work is financially supported by the National Natural Science Foundation of China (Grant no. 21176260 and 21376268), Taishan Scholar Foundation (No. ts20130929) and Fundamental Research Funds for the Central Universities (15CX06050A).

Appendix A. Supplementary material

Supplementary data associated with this article can be found in the online version at http://dx.doi.org/10.1016/j.matlet.2015.11.127.

References

[1] S. Wei, Q. Wang, J. Zhu, L. Sun, H. Lin, Z. Guo, Nanoscale 3 (2011) 4474–4502.
[2] Y. Wang, J. Zhang, L. Liu, C. Zhu, X. Liu, Q. Su, Mater. Lett. 75 (2012) 95–98.
[3] B. Jiang, X.L. Yang, X. Li, D.Q. Zhang, J. Sol–Gel Sci. Technol. 66 (2013) 504–511.
[4] C. Xu, X. Wei, Z. Ren, Y. Wang, G. Xu, G. Shen, G. Han, Mater. Lett. 63 (2009) 2194–2197.
[5] P. Wang, J. Wu, Y. Ao, C. Wang, J. Hou, J. Qian, Mater. Lett. 65 (2011) 3278–3280.
[6] S.Q. Liu, N. Zhang, Z.R. Tang, Y.J. Xu, ACS Appl. Mater. Interface 4 (2012) 6378–6385.
[7] S. Li, J.T. Zheng, W.L. Yang, Y.C. Zhao, Mater. Lett. 61 (2007) 4784–4786.
[8] H. Wang, Q. Xu, X. Zheng, J. Nanopart. Res. 16 (2014) 1–15.
[9] T. Sugimoto, X.P. Zhou, J. Colloid Interface Sci. 252 (2002) 347–353.
[10] X.F. Bian, K.Q. Hong, L.Q. Liu, M.X. Xu, Appl. Surf. Sci. 280 (2013) 349–353.
[11] G. Cui, W. Wang, M. Ma, M. Zhang, X. Xia, F. Han, Chem. Commun. 49 (2013) 6415–6417.